Project: Near Singular Integration

Sanjida Yeasmin, Jonathan Engle and, Lasitha Gunasekara

April 24th, 2025

Introduction

In many applications of computational science and engineering, evaluating boundary integrals accurately is crucial. Standard numerical quadrature schemes often perform well when the evaluation point is far from the boundary. However, when the evaluation point approaches the boundary surface, the integrand becomes sharply peaked, causing traditional quadrature methods to fail. This phenomenon is referred to as *near singular behavior*.

Near singular integration refers to the numerical evaluation of integrals where the kernel or the integrand exhibits large variations due to the close proximity of the evaluation point to the integration domain. Although the integrals remain mathematically well-defined and finite, standard quadrature rules experience significant accuracy loss because they cannot resolve the steep gradients effectively.

Accurate treatment of near singular integrals is critical in many fields, including:

- Boundary Integral Methods (BIM) for fluid dynamics, elasticity, and electro magnetics
- Particle simulations and Stokes flow computations
- Fast multiple and QBX (Quadrature by Expansion) methods

Several specialized strategies have been developed to address near singular integration challenges, such as:

- Local interpolation and re parametrization techniques
- Singular or nearly singular quadrature corrections
- Adaptive mesh refinement near boundaries
- Analytical regularization and expansion-based approaches

This project explores some numerical methods designed to improve the accuracy of integral evaluations in the presence of near singular behavior, aiming to balance efficiency and precision for practical scientific computing applications.

Literature Review

[Beale and Tlupova(2024)] replaces the singular kernel for the single and/ or double layer potentials with a regularized version having a length parameter δ to control the discretization error. The authors then discuss the different choices for this δ, for convergence as the step size approaches zero i.e. $h \to 0$, the authors choose δ to be proportional to h^q where $q < 1$ to ensure that the discretization error is dominated by the regularization error. Finally, they find that a choice of $q = 4/5$ you obtain an error on the order of $\mathcal{O}(h^4)$. The paper discusses many different topics, for our purposes we focus on the double layer potential

$$\mathcal{D}(\mathbf{y}) = \int_\Gamma \frac{\partial G(\mathbf{x}-\mathbf{y})}{\partial \mathbf{n}(\mathbf{x})} g(\mathbf{x}) dS(\mathbf{x}) \tag{1}$$

Where using Green's identities, above can be rewritten as:

$$\mathcal{D}(\mathbf{y}) = \int_{\Gamma} \frac{\partial G(\mathbf{x}-\mathbf{y})}{\partial \mathbf{n}(\mathbf{x})} \left[g(\mathbf{x}) - g\left(\mathbf{x}_0\right)\right] dS(\mathbf{x}) + \chi(\mathbf{y}) g\left(\mathbf{x}_0\right) \tag{2}$$

Where $\mathbf{x}_0$ is the point closest to the boundary Γ, the authors set $\chi = 0$ for interior, $\chi = 1$ for the exterior and $\chi = 1/2$ for on the boundary Γ. To regularize the authors replace ∇D with the gradient of the smooth function G_δ obtaining

$$\nabla G_\delta\left(\mathbf{r}\right) = \nabla G(\mathbf{r}) s_2\left(\frac{|\mathbf{r}|}{\delta}\right) = \frac{\mathbf{r}}{4\pi|\mathbf{r}|^3} s_2\left(\frac{|\mathbf{r}|}{\delta}\right) \tag{3}$$

Where:

$$s_2(r) = \operatorname{erf}(r) - \left(\frac{2}{\sqrt{\pi}}\right) r e^{-r^2}, \tag{4}$$

$$\operatorname{erf}(x) = \frac{2}{\sqrt{\pi}} \int_0^x e^{-t^2} dt \tag{5}$$

Leaving us with:

$$\mathcal{D}_\delta(\mathbf{y}) = \int_{\Gamma} \frac{\mathbf{r}\cdot\mathbf{n}(\mathbf{x})}{4\pi||\mathbf{r}|^3} s_2\left(\frac{|\mathbf{r}|}{\delta}\right) [g(\mathbf{x}) - g(\mathbf{x}_0)] dS(\mathbf{x}) + \chi(\mathbf{y}) g(\mathbf{x}_0), \quad \mathbf{r} = \mathbf{x} - \mathbf{y} \tag{6}$$

In the [Ioakimidis et al.(1991)Ioakimidis, Papadakis, and Perdios] paper they discuss 3 main ideas for solving this problem. First is, the direct method approach using elementary quadrature rule with n nodes

$$\int_{\mathbb{C}} g(t) dt = \sum_{j=1}^{n} A_{jn} g\left(t_{jn}\right) + E_n(g) \tag{7}$$

Where A_{jn} is the basis, $g\left(t_{jn}\right)$ is our interpolated values and $E_n(g)$ is the correction term. For our purposes we can think of this elementary method as the Trapezoidal method which we have used in class. Second, is the indirect approach where the authors use of Taylor Series for points far away from the singularity

$$f(z) = \sum_{j=0}^{\infty} a_j \left(z - z_0\right)^j \tag{8}$$

a_j is then computed by

$$a_j = \frac{1}{j!} f^{(j)}\left(z_0\right) = \frac{1}{2\pi i} \int_C \frac{f(t)}{\left(t - z_0\right)^{j+1}} dt, \quad j = 0, 1, \ldots \tag{9}$$

Where the point z is substituted by the point z_0.

$$f^{(m)}(z) = \sum_{j=0}^{\infty} a_j j(j-1)\ldots(j-m+1) z^{j-m}, \quad m = 0, 1, \ldots \tag{10}$$

Lastly, the authors utilize of Cauchy's Theorem

$$\int_{\mathbb{C}} g(t) dt = 0 \tag{11}$$

where $g(z)$ is analytic and without poles. This is then applied to:

$$f(z) = \frac{1}{2\pi i} \int_{\mathbb{C}} \frac{f(t)}{t - z} \tag{12}$$

$$f^{(m)}(z) = \frac{m!}{2\pi i} \int_{\mathbb{C}} \frac{f(t)}{(t-z)^{m+1}} dt, \quad m = 1, 2, \ldots \tag{13}$$

n	Method A: $f(z) - f_n(z)$	Method C: $f(z) - f_n(z)$
4	$(-3.0042 - i3.5419)E + 0$	$(-4.1124 - i0.7238)E - 2$
8	$(-1.2459 - i1.5693)E + 0$	$(-2.2418 - i0.2219)E - 4$
16	$(-4.9821 - i6.2782)E - 1$	$(-1.8076 - i0.0954)E - 11$
32	$(-1.5340 - i1.9331)E - 1$	absolutely $< 1.0E - 15$
64	$(-2.5347 - i3.1941)E - 2$	"
128	$(-0.9556 - i1.2042)E - 3$	"
256	$(-1.4646 - i1.8456)E - 6$	"

Figure 1: Numerical results for errors in $f(z)$ and $f'(z)$ with $f(z) = e^z$ by using the trapezoidal rule with $n = 2^q$ for an elliptic contour with semi-axes at $a = 2, b = 1$ and centered at 0, also $z = 0.9i$.

This method does perform well as seen in Figure 1. As we can see the utilization of this method converges to machine precision much faster than the simple method.

[Klöckner et al.(2013)Klöckner, Barnett, Greengard, and O'Neil] aims to introduce and validate a novel numerical approach, the Quadrature by Expansion (QBX) method, for the accurate evaluation of layer potentials with singular, weakly singular, or nearly singular kernels in integral equation methods. The objective is to overcome the challenges associated with evaluating boundary integrals that arise in the application of integral equation methods for solving partial differential equations.

[Zhu and Veerapaneni(2022)] introduces a high-order accurate numerical algorithm for evaluating the double layer potential (DLP) of the Laplace equation in three dimensions, particularly focusing on the challenging evaluation problem, computing layer potentials at points very close to the surface over which they are defined. This is a common issue in boundary integral methods for elliptic PDEs, where standard quadrature fails due to the near-singular behavior of the integrand.

Nearly Singular Integration: [Biros et al.(2006)Biros, Ying, and Zorin]

To evaluate the boundary integral

$$(D\phi)(x) = \int_\Gamma D(x,y)\phi(y)\,dy$$

at a point $x \in \Omega$, we partition the domain Ω based on the distance from x to the boundary Γ. The partition depends on the discretization parameter $h \ll 1$, and allows us to apply specialized strategies in each subregion to handle near-singular behavior of the kernel $D(x, y)$.

- **Region Ω_0 (Well-Separated):**
  Defined as $\Omega_0 = \{x \in \Omega : \text{dist}(x, \Gamma) > \sqrt{h}\}$.
  The kernel $D(x, y)$ is smooth in this region. We use the trapezoidal rule directly on the boundary quadrature points, possibly accelerated with the Fast Multiple Method (FMM).

- **Region Ω_1 (Intermediate):**
  Defined as $\Omega_1 = \{x \in \Omega : h < \text{dist}(x, \Gamma) \leq \sqrt{h}\}$.
  The kernel is sharply peaked and the standard trapezoidal rule is not accurate enough. To address this, the boundary data ψ_k is resampled on a finer Cartesian grid of spacing $h^{3/2}$ using FFTs. The integral is then evaluated with a trapezoidal rule on the refined grid.

- **Region Ω_2 (Nearest):**
  Defined as $\Omega_2 = \{x \in \Omega : \text{dist}(x, \Gamma) \leq h\}$.
  In this region, the kernel becomes nearly singular. For such points:

1. Find a point $x_0 \in \Gamma$ such that the direction $x - x_0$ is approximately aligned with the surface normal at x_0.
2. Construct a set of points $\{x_\ell\}_{\ell=1}^{L}$ along the line from x_0 toward x.
3. Evaluate $D\phi(x_\ell)$ at each x_ℓ using the methods for Ω_1 or Ω_0.
4. Interpolate the value $D\phi(x)$ using 1D Lagrange interpolation from the values at $\{x_\ell\}$.

This domain decomposition and quadrature strategy ensure that high order accuracy is maintained uniformly throughout the domain.

Quadrature by expansion: A new method for the evaluation of layer potentials: [Klöckner et al.(2013)Klöckner, Barnett, Greengard, and O'Neil]

The method is designed to evaluate layer potentials, such as single- and double-layer potentials, which involve integrals with singular or weakly singular kernels. These potentials are defined as:

$$S\sigma(x) := \int_\Gamma G\left(x, x'\right) \sigma\left(x'\right) dx',$$
$$D\mu(x) := \int_\Gamma \frac{\partial G}{\partial \hat{n}_{x'}}\left(x, x'\right) \mu\left(x'\right) dx'$$

for target points x on a closed, smooth contour $\Gamma \subset \mathbb{R}^2$, where G is the Green's function for an underlying elliptic PDE and $\hat{n}_{x'}$ denotes the outward unit normal at x'. In the case of the double layer potential, it is typically the principal value of $D\mu$ that is desired for $x \in \Gamma$.

- **Smoothness Assumption:** QBX relies on the principle that the layer potentials are smooth away from the boundary. Although the integral kernels may be singular, the resulting potential field is smooth in the interior Ω^- and exterior Ω^+ domains.
- **Local Expansion:** For a target point x on the boundary Γ , a nearby off-surface point c is chosen. The potential is then approximated by a local expansion (e.g., a series in Bessel functions for the Helmholtz equation) around c . For the Helmholtz equation, the local expansion takes the form:

  $$\phi(x) = \sum_{l=-\infty}^{\infty} \alpha_l J_l(k\rho) e^{-il\theta}$$

  Where: ρ, θ are polar coordinates of the target x with respect to the expansion center c .J_l are Bessel functions of order l.
- **Coefficient Computation:** The coefficients α_l in the local expansion are computed by integrating the kernel multiplied by the density function.For each expansion center c and for $l = -p, -p+1, ..., p$, compute the coefficients α_l using a high-order quadrature rule:
  Single layer:

  $$\alpha_l = \frac{i}{4} \int_\Gamma H_l^{(1)}(k|x' - c|) e^{il\theta'} \sigma(x') dx'$$

  Double layer:

  $$\alpha_l^D = \frac{i}{4} \int_\Gamma \frac{\partial}{\partial \hat{n}_{x'}} H_l^{(1)}(k|x' - c|) e^{il\theta'} \mu(x') dx'$$

  Where: $H_l^{(1)}$ are Hankel functions of the first kind. $(|x' - c|, \theta')$ are polar coordinates of x' with respect to c. These integrals are evaluated using standard high-order quadrature rules for smooth functions, such as Gauss-Legendre quadrature or the trapezoidal rule.
- **Evaluation:** The layer potential at the boundary point x is approximated by evaluating the local expansion at x .
- **Multiple Centers:** To evaluate the potential over the entire boundary, multiple expansion centers are distributed near the boundary, each covering a local region.

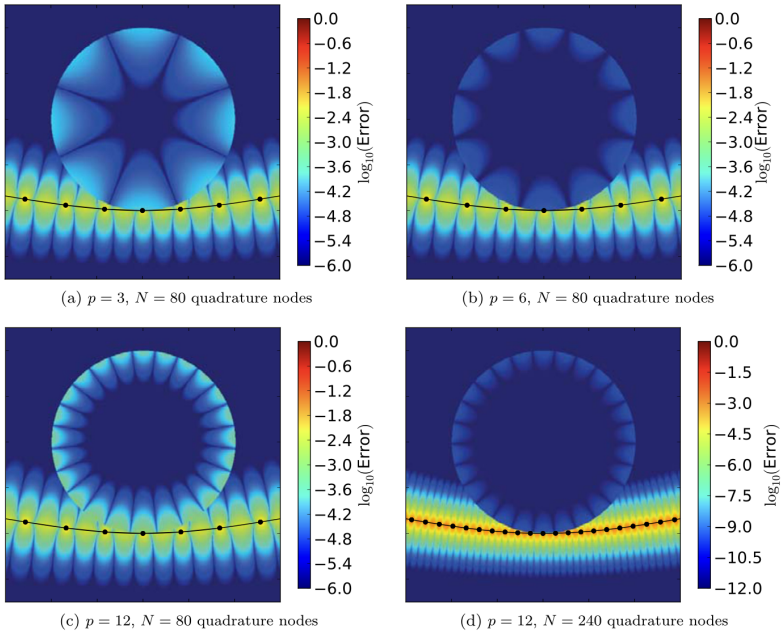

(a) $p = 3$, $N = 80$ quadrature nodes

(b) $p = 6$, $N = 80$ quadrature nodes

(c) $p = 12$, $N = 80$ quadrature nodes

(d) $p = 12$, $N = 240$ quadrature nodes

Fig. 3. The potential $S\sigma$ is computed using the trapezoidal rule Γ with either $N = 80$ or $N = 240$ points, except in a disk of radius $|c - x|$ centered at an off-surface point c that lies in the "high-accuracy" region of the trapezoidal rule (here, approximately $3h$ away from the curve in (a), (b), and (c)). Only a portion of the boundary Γ is plotted, and x is the point where the disk and Γ are tangent. We plot the error in the disk using various expansion orders p and numbers of quadrature nodes.

High order close evaluation of Laplace layer potential: A differential geometric approach: [Zhu and Veerapaneni(2022)]

The double-layer potential (DLP) for Laplace equation given by

$$\mathcal{D}[\mu]\left(\boldsymbol{r}'\right) = \int_{\mathcal{M}} \frac{\partial G\left(\boldsymbol{r}' - \boldsymbol{r}\right)}{\partial \boldsymbol{n}_{\boldsymbol{r}}} \mu(\boldsymbol{r}) dS_{\boldsymbol{r}}$$

where $G\left(\boldsymbol{r}' - \boldsymbol{r}\right) = 1/4\pi \left|\boldsymbol{r}' - \boldsymbol{r}\right|$ is Green's function for the Laplace equation, $\mu(\boldsymbol{r})$ is a density function, $\mathcal{M}$ is a closed two-dimensional manifold in $\mathbb{R}^3$, and $\boldsymbol{n}_{\boldsymbol{r}}$ is its normal.

Mathematical Preliminaries:

- Exterior algebra provides the formal language to express and manipulate differential forms. Alternating k-forms on a vector space V are multilinear antisymmetric maps:

  $$\omega(v_1, \ldots, v_k) \in \mathrm{Alt}^k(V).$$

  The wedge product of forms $\omega \in \mathrm{Alt}^k(V)$ and $\eta \in \mathrm{Alt}^l(V)$ is given by:

  $$(\omega \wedge \eta)(v_1, \ldots, v_{k+l}) = \sum_{\sigma \in Sh(k,l)} \mathrm{sgn}(\sigma)\omega(v_{\sigma(1)}, \ldots, v_{\sigma(k)})\eta(v_{\sigma(k+1)}, \ldots),$$

  ensuring antisymmetry and bilinearity.

- A differential k-form ω on a manifold $\mathcal{M}$ assigns a k-form to every point. The exterior derivative d raises form degree and satisfies:

  $$d(\omega \wedge \eta) = d\omega \wedge \eta + (-1)^k \omega \wedge d\eta.$$

- The double-layer potential (DLP) solves Dirichlet BVPs for the Laplace equation:

$$u(\mathbf{r}') = \mathcal{D}[\mu](\mathbf{r}'), \quad \mathcal{D}[\mu](\mathbf{r}') = \int_{\mathcal{M}} \frac{(\mathbf{r}' - \mathbf{r}) \cdot \mathbf{n}_{\mathbf{r}}}{4\pi|\mathbf{r}' - \mathbf{r}|^3} \mu(\mathbf{r})\, dS_{\mathbf{r}}.$$

  This can be expressed using exterior 2-forms for componentwise analysis:

$$\frac{(x' - x)\mu}{4\pi|\mathbf{r}' - \mathbf{r}|^3} dy \wedge dz + \frac{(y' - y)\mu}{4\pi|\mathbf{r}' - \mathbf{r}|^3} dz \wedge dx + \frac{(z' - z)\mu}{4\pi|\mathbf{r}' - \mathbf{r}|^3} dx \wedge dy$$

Density Approximation and Exact Form Construction

- Stokes' theorem converts 2-form integrals to 1-form contour integrals:

$$\int_D d\omega = \int_{\partial D} \omega.$$

  To use this requires $d\omega = \alpha$, i.e., α is exact. From Poincaré's Lemma, any closed 2-form α (i.e., $d\alpha = 0$) is locally exact. **Lemma 3.3** gives explicit construction:

$$\omega = \left(\int_0^1 (tzg_2 - tyg_3) dt \right) dx + \left(\int_0^1 (txg_3 - tzg_1) dt \right) dy + \left(\int_0^1 (tyg_1 - txg_2) dt \right) dz.$$

  Lemma 3.3 Consider a compact oriented two dimensional manifold D in $\mathbb{R}^3$. Let

$$\alpha = g_1(\boldsymbol{r}) dy \wedge dz + g_2(\boldsymbol{r}) dz \wedge dx + g_3(\boldsymbol{r}) dx \wedge dy$$

  be a differential 2-form on D. If $d\alpha = 0$ (i.e., $\nabla \cdot (g_1, g_2, g_3) = 0$), then α is an exact form on D; i.e., there exists some 1 -form ω such that $d\omega = \alpha$.

- Define a quaternion $g = g_0 + g_1\mathbf{i} + g_2\mathbf{j} + g_3\mathbf{k}$. The kernel and density product is expressed using quaternionic multiplication:

$$\alpha = \frac{(\mathbf{r}' - \mathbf{r}) \cdot \mathbf{n}(\mathbf{r})}{|\mathbf{r}' - \mathbf{r}|^3} f(\mathbf{r}) dS_{\mathbf{r}}.$$

  Lemma 3.4: If $\mathbf{f} = \nabla\phi$, $\mathbf{g} = \nabla\psi$ for harmonic functions, the scalar and vector parts of the quaternion product are exact differential forms. This enables a systematic reduction to 1-form using Stokes.

Numerical Scheme

- Surface $\mathcal{M}$ is split into triangular patches D.
- On each patch, μ is approximated via harmonic polynomials ϕ_k:

$$\mu(\mathbf{r}) \approx \sum_{k,l} f_{k,l}(\mathbf{r}) c_{k,l}, \quad f_{k,l} = \nabla\phi_k \text{ in quaternionic form.}$$

- Collocation at Gauss–Legendre nodes gives a linear system to solve for $c_{k,l}$.
- Construct quaternionic 2-form:

$$\alpha_i^{(k,l)} = \frac{\mathbf{q}_i^{(k,l)}(\mathbf{r}', \mathbf{r}) \cdot \mathbf{n}(\mathbf{r})}{|\mathbf{r}' - \mathbf{r}|^3} dS_{\mathbf{r}}$$

- Using Lemma 3.3, convert $\alpha_i^{(k,l)}$ to 1-forms $\omega_i^{(k,l)}$.
- Evaluate

$$\int_{\partial D} \omega_i^{(k,l)}$$

  numerically using high-order smooth quadrature.

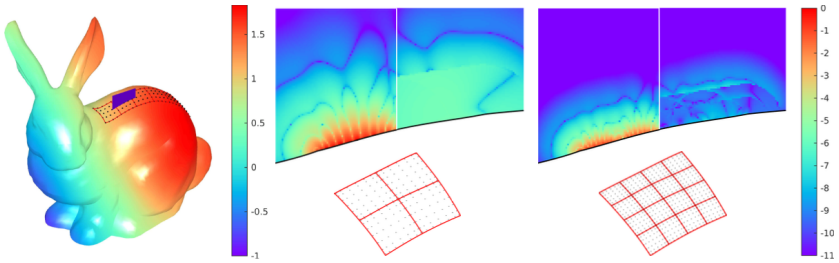

FIG. 1. *One of the key advantages of the close evaluation scheme developed in this paper is its ease of handling arbitrary meshes. Here, we demonstrate its performance on the Stanford bunny triangulation data* [27]. *We used the interactive sketch-based quadrangulation method of* [24] *to create high-quality quad remeshings locally as shown on the top of the bunny. We evaluate the DLP at targets that are located arbitrarily close to the surface as shown on top in blue color. The surface is colored by the density function* μ*, which was set as* $\mu(x, y, z) = e^{xy} - 1 + x + \sin(x^4 + 1/2y^3) + y - 1/2y^2 + 1/5y^6 + z$. *Middle and right: Given this setup, we demonstrate the performance of the new scheme by considering one of the quads, successively refining it twofold and visualizing the errors due to direct evaluation of DLP via the high-order smooth quadrature rule (left half) and the new close evaluation scheme (right half). We note that, while the errors stagnate in a band close to the surface in the case of smooth quadrature, the new scheme achieves uniform accuracy up to* 10 *digits. This is a self-convergence test compared with a reference solution obtained on an* 8×8 *panel refinement of the quad. More details on this experiment are provided in section* 5.

Convergence

- On analytic test functions, the scheme achieves **7th-order convergence**.
- Close evaluation accuracy does not degrade near the boundary — errors remain small and uniform.
- On complex geometries, the method handles unstructured meshes robustly.
- Achieves up to **10-digit accuracy** for targets arbitrarily close to the surface.

Description of the methods : [Biros et al.(2006)Biros, Ying, and Zorin]

Limitations of the Nearly Singular Method

- **Requires smooth surfaces:** The method assumes that the boundary surface Γ is infinitely smooth. It is not well-suited for domains with corners, edges, or non-smooth parameterizations.
- **Interpolation cost increases:** In the nearest region Ω_2, evaluating the integral at off surface points and performing high order Lagrange interpolation becomes computationally expensive for large L or fine grids.
- **Does not handle true singularities:** This method is designed for *nearly* singular integrals (when $x \notin \Gamma$ but is close). For singular integrals (when $x \in \Gamma$), separate singular quadrature schemes are still required.
- **Not adaptive:** The quadrature is based on uniform grids and fixed spacing h, making it less effective for adaptive refinement or nonuniform discretizations.
- **Limited to standard kernels:** The method is optimized for classical kernels (e.g., Laplace and Stokes double layers).
- **No built-in error control:** The method does not include an automatic error estimator. High accuracy is achieved only if parameters (e.g., interpolation order, up-sampling factor) are properly chosen.

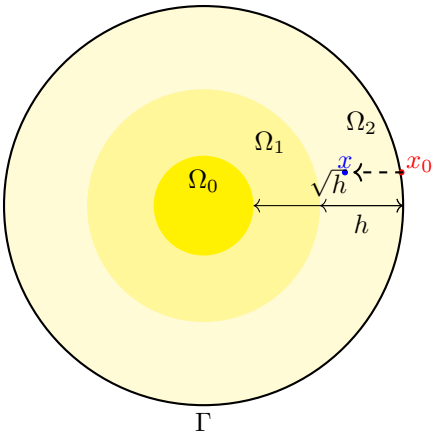

(a) Domain partitioning.

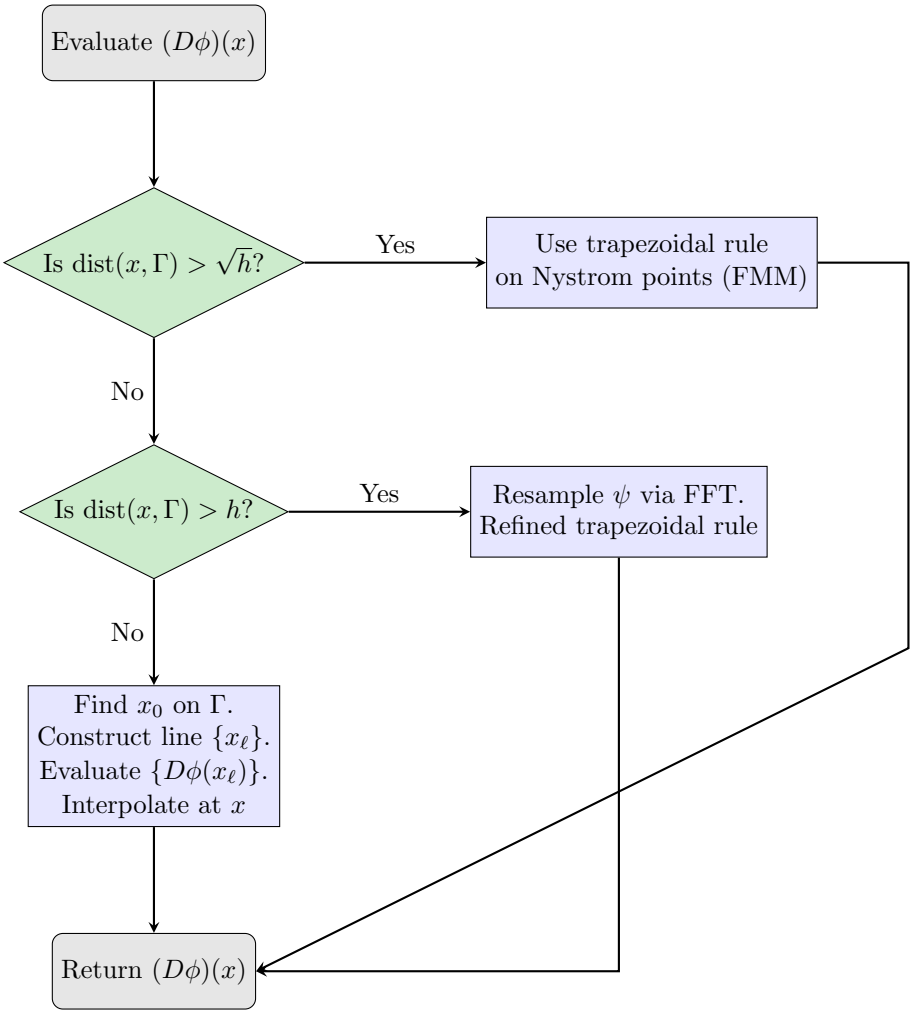

(b) Strategy for evaluating $(D\phi)(x)$

Figure 2: Partitioning of the domain and corresponding evaluation strategies.

Numerical results

Benchmark Results from [Biros et al.(2006)Biros, Ying, and Zorin]

To evaluate the accuracy and efficiency of the nearly singular integration method, we include results from the original paper by Biros, Ying, and Zorin. These tests were performed for both Laplace and Stokes double

layer potentials using exact analytical solutions. The tables below summarize the convergence behavior of the singular and nearly singular quadrature methods as the discretization is refined.

Table 1: Singular and nearly singular integration of the Laplace kernel.

h	N	T_s	Error_s	Ratio_s	T_n	Error_n	Ratio_n
0.1000	1688	1.660e+00	7.551e-04	1.027e+01	5.100e-01	5.259e-04	7.203e+00
0.0500	5480	8.980e+00	7.352e-05	1.348e+01	2.950e+00	7.301e-05	1.208e+01
0.0250	20736	6.928e+01	5.456e-06	7.406e+00	2.229e+01	6.046e-06	7.683e+00
0.0125	78792	4.636e+02	7.367e-07	–	1.039e+02	7.869e-07	–

Table 2: Singular and nearly singular integration of the Stokes kernel.

h	N	T_s	Error_s	Ratio_s	T_n	Error_n	Ratio_n
0.1000	2400	2.410e+00	3.489e-04	7.977e+00	4.460e+00	5.072e-04	9.916e+00
0.0500	9600	1.621e+01	4.374e-05	1.575e+01	2.113e+01	5.115e-05	1.614e+01
0.0250	38400	1.228e+02	2.778e-06	1.156e+01	1.664e+02	3.169e-06	1.319e+01
0.0125	149784	9.142e+02	2.403e-07	–	1.333e+03	2.403e-07	–

Interpretation: The results in Tables 1 and 2 demonstrate the high-order convergence of the nearly singular quadrature method. As h decreases, both singular and nearly singular errors decrease rapidly. The nearly singular integration maintains accuracy even when evaluation points are very close to the boundary.

Conclusion and Future Work

Here we have studied a survey of methods pertaining to solving these near singular integration issues. A few expansions which we wish to implement in the future are:

1. We will implement the three-region method, regularization method, and the differential geometric approach discussed.
2. We will compare all of the methods and perform a detailed convergence a analysis.
3. We aim to conduct a comprehensive review of the methods discussed in this study.
4. Try additional functions to study convergence and analysis.
5. Possibly use them in our own research

References

[Beale and Tlupova(2024)] J. Thomas Beale and Svetlana Tlupova. Extrapolated regularization of nearly singular integrals on surfaces. *Advances in Computational Mathematics*, 50(4):61, 2024. doi: 10.1007/s10444-024-10161-4. URL `https://doi.org/10.1007/s10444-024-10161-4`.

[Biros et al.(2006)Biros, Ying, and Zorin] George Biros, Lexing Ying, and Denis Zorin. A fast algorithm for the evaluation of nearly-singular layer potentials. *Journal of Computational Physics*, 212(1):132–156, 2006.

[Ioakimidis et al.(1991)Ioakimidis, Papadakis, and Perdios] N. I. Ioakimidis, K. E. Papadakis, and E. A. Perdios. Numerical evaluation of analytic functions by cauchy's theorem. *BIT Numerical Mathematics*, 31(2):276–285, 1991. doi: 10.1007/BF01931287. URL `https://doi.org/10.1007/BF01931287`.

[Klöckner et al.(2013)Klöckner, Barnett, Greengard, and O'Neil] Andreas Klöckner, Alexander Barnett, Leslie Greengard, and Michael O'Neil. Quadrature by expansion: A new method for the evaluation of layer potentials. *Journal of Computational Physics*, 252:332–349, 2013. ISSN 0021-9991. doi: https://doi.org/10.1016/j.jcp.2013.06.027. URL `https://www.sciencedirect.com/science/article/pii/S0021999113004579`.

[Zhu and Veerapaneni(2022)] Hai Zhu and Shravan Veerapaneni. High-order close evaluation of laplace layer potentials: A differential geometric approach. *SIAM Journal on Scientific Computing*, 44(3):A1381–A1404, 2022. doi: 10.1137/21M1423051. URL `https://doi.org/10.1137/21M1423051`.